FISEVIER

Contents lists available at ScienceDirect

Acta Biomaterialia

journal homepage: www.elsevier.com/locate/actabiomat



Full length article

Robust antigen-specific tuning of the nanoscale barrier properties of biogels using matrix-associating IgG and IgM antibodies



Jennifer L. Schiller a, Allison Marvin a, Justin D. McCallen a, Samuel K. Lai a,b,c,*

- a Division of Pharmacoengineering and Molecular Pharmaceutics, Eshelman School of Pharmacy, University of North Carolina at Chapel Hill, Chapel Hill, NC 27599, United States
- b UNC/NCSU Joint Department of Biomedical Engineering, University of North Carolina at Chapel Hill, Chapel Hill, NC 27599, United States
- ^c Department of Microbiology & Immunology, University of North Carolina at Chapel Hill, Chapel Hill, NC 27599, United States

ARTICLE INFO

Article history:
Received 23 September 2018
Received in revised form 11 March 2019
Accepted 12 March 2019
Available online 14 March 2019

Keywords:
Basement membrane
Extracellular matrix
Antibodies
Laminin
Particle tracking
PEG

ABSTRACT

Biological hydrogels (biogels) are selective barriers that restrict passage of harmful substances yet allow the rapid movement of nutrients and select cells. Current methods to modulate the barrier properties of biogels typically involve bulk changes in order to restrict diffusion by either steric hindrance or direct high-affinity interactions with microstructural constituents. Here, we introduce a third mechanism, based on antibody-based third party anchors that bind specific foreign species but form only weak and transient bonds with biogel constituents. The weak affinity to biogel constituents allows antibody anchors to quickly accumulate on the surface of specific foreign species and facilitates immobilization via multiple crosslinks with the biogel matrix. Using the basement membrane Matrigel® and a mixture of laminin/entactin, we demonstrate that antigen-specific, but not control, IgG and IgM efficiently immobilize a variety of individual nanoparticles. The addition of *Salmonella typhimurium*-binding IgG to biogel markedly reduced the invasion of these highly motile bacteria. These results underscore a generalized strategy through which the barrier properties of biogels can be readily tuned with molecular specificity against a diverse array of particulates.

Statement of Significance

Biological hydrogels (biogels) are essential in living systems to control the movement of cells and unwanted substances. However, current methods to control transport within biogels rely on altering the microstructure of the biogel matrix at a gross level, either by reducing the pore size to restrict passage through steric hindrance or by chemically modifying the matrix itself. Both methods are either nonspecific or not scalable. Here, we offer a new approach, based on weakly adhesive third-party molecular anchors, that allow for a variety of foreign entities to be trapped within a biogel simultaneously with exceptional potency and molecular specificity, without perturbing the bulk properties of the biogel. This strategy greatly increases our ability to control the properties of biogels at the nanoscale, including those used for wound healing or tissue engineering applications.

 $\ensuremath{\text{@}}$ 2019 Acta Materialia Inc. Published by Elsevier Ltd. All rights reserved.

1. Introduction

Biological hydrogels (biogels) are ubiquitous in living systems. In addition to providing essential structural support and mechanical function, such as lubrication in copulation and anchoring of cells to tissues [1–3], biogels serve as a selective barrier that can

E-mail address: lai@unc.edu (S.K. Lai). URL: http://www.lailab.com (S.K. Lai).

impede diffusion of unwanted materials yet allow the rapid movement of nutrients and select cells [2,4–6]. The biochemical composition of biogels, such as Matrigel® [7] and mucus [3], is generally highly conserved. Matrigel®, basement membrane extract derived from the Engelbreth-Holm Swarm sarcoma, is comprised of 60% laminin, 30% collagen type IV, 8% entactin/nidogen, and 2% heparan sulfate, growth factors, and salts [8,9]. This implies the biogel constituents are unlikely to adhesively capture the full diversity of foreign species, particularly since some pathogens have evolved to evade adhesive interactions with biogel matrices [2,10,11]. Thus, biogels are generally assumed to pose only a steric barrier to diffusion based on pore size, which varies based on the concentration of

^{*} Corresponding author at: Division of Pharmacoengineering and Molecular Pharmaceutics, University of North Carolina at Chapel Hill, Marsico 4213, 125 Mason Farm Road, United States.

their matrix constituents and cannot immobilize species smaller than the mesh spacing. Indeed, steric trapping of micro- and nanoparticulates in Matrigel® and other highly glycosylated biologically derived hydrogels is well established [12-14]. Consequently, to tune the barrier properties of biogels, the predominant strategies are to either (i) alter the pore sizes of the gel matrix and impede transit through changing steric hindrance [2,15] or (ii) conjugate specific motifs to the gel itself that in turn bind foreign species [16-20]. Both approaches involve substantial drawbacks. Bulk changes to the matrix microstructure, either by changing the crosslinker concentration in covalently linked gels or by relying on environmental stimuli (e.g. light or enzymes, respectively) to polymerize or degrade matrix constituents [20-25], only facilitate selectivity based on size and are generally irreversible. Alternatively, covalent crosslinking of antigen-specific molecules to the matrix [16-19,25] is cumbersome in practice, is limited in the number of species that can be simultaneously immobilized, and may not efficiently immobilize diffusive species [26].

We believe the ideal method to tune the barrier properties of biogels should be antigen-specific and does not involve indiscriminate changes to the gel microstructure or direct chemical alterations of the matrix. These design requirements motivated us to explore the use of highly adaptive third-party anchors that can bind nanoparticulates with molecular specificity and crosslink them to matrix constituents. Due to the ability of Fab domains to undergo somatic hypermutation and affinity maturation to bind specific antigens with nanomolar affinities, antibodies represent a promising class of crosslinkers. We sought here to determine whether antibody Fc, which are highly conserved, would possess the appropriate affinity with biogel constituents to enable potent tuning of the barrier properties.

2. Materials and methods

2.1. Preparation of PEG-coated nanoparticles

To produce PEGylated nanoparticles (PS-PEG), we covalently modified 200 nm fluorescent, carboxyl-modified polystyrene beads (PS-COOH; Invitrogen) with 2 kDa methoxy polyethylene glycol amine (PEG; Sigma) via a carboxyl-amine reaction, as published previously [27,28]. Particle size and ζ -potential were determined by dynamic light scattering and laser Doppler anemometry, respectively, using a Zetasizer Nano ZS (Malvern Instruments, Southborough, MA). Size measurements were performed at 25 °C at a scattering angle of 90°. Samples were diluted in 10 mM NaCl solution, and measurements were performed according to instrument instructions. PEG conjugation was also confirmed by a near-neutral ζ -potential [27]. Dense PEG grafting (>1 PEG/nm²) was further verified using the fluorogenic compound 1-pyrenyldiazomethane (PDAM) to quantify residual unmodified carboxyl groups on the polystyrene beads [28].

2.2. Preparation of Matrigel®, laminin, and collagen for microscopy

A mixture of the following was added to a custom-made microvolume ($\sim 10~\mu L$) glass chamber slide: (i) growth-factor reduced Matrigel® (MG; Corning), high-concentration laminin/entactin (LAM; Corning), or mouse collagen IV (COL; Sigma); (ii) BSA (Sigma); (iii) Eagle's Minimum Essential Medium (EMEM, Lonza BioWhittacker); (iv) fluorescent PS-COOH (Ex: 505 nm, Em: 515 nm) and PS-PEG (Ex: 625 nm, Em: 645 nm) nanoparticles; and (v) different Ab. The mixture was incubated at 37 °C for 45 min in a custom hydration chamber, then sealed and incubated for another 30 min prior to microscopy. Final concentrations of reagents in slides were as follows: 2.2 mg/mL MG, 1 mg/mL BSA,

 ${\sim}4.3^*10^8$ beads/mL for both PEG- and COOH-modified nanoparticles, antibody as listed, EMEM, q.s. In LAM experiments, the final concentration of LAM was 1.5 mg/mL (comparable to the concentration of laminin in 2.2 mg/mL MG). In COL experiments, gel did not set at the concentration of laminin corresponding to that in 2.2 mg/mL of MG, so a final concentration of 3 mg/mL of COL was required. Lyophilized COL was resuspended in 0.25% v/v acetic acid and neutralized with 1 M NaOH to facilitate gelation. Trapping of PS-COOH beads in MG was used as an internal control in all microscopy experiments as a measure of complete polymerization of MG constituents.

2.3. Antibodies

Anti-PEG IgG₁ (CH2074 except excess biotin experiment, which used CH2076, Silver Lake Research) and anti-PEG IgM (AGP4, IBMS) were used as test Ab and anti-Biotin IgG₁ (Z021, ThermoFisher) and anti-Vancomycin IgM (2F10, Santa Cruz) were used as control Ab. All native Ab were used as is provided by the manufacturer. To prepare deglycosylated Ab, N-glycans on anti-PEG IgG and IgM were removed with rapid non-reducing PNGase F enzyme (New England Biolabs) according to the manufacturer's protocol. The deglycosylation reaction was confirmed with two NuPAGE 4-12% Bis-Tris gels (Novex) in MOPS buffer. The first gel was transferred to a nitrocellulose membrane (Novex) with a Semi-Dry Blotter (Novex), blocked with carbo-free buffer (Vector Labs), labeled overnight at 4 °C in 2 μg/mL biotinylated concavalin A (Vector), and probed with anti-biotin peroxidase (Vector) before imaging with Clarity Western Blot ECL Substrate (BioRad) in a FluorChemE unit (Cell Biosciences). The second gel was silver stained with Pierce Silver Stain Kit (Thermo Scientific) and imaged with the same unit. The remaining deglycosylated IgG and IgM was buffer-exchanged into PBS using 50 MWCO spin-x columns (Corning) and quantified based on A280.

2.4. High-resolution multiple particle tracking

Using an EMCCD camera (Evolve 512: Photometrics, Tucson, AZ) affixed to an inverted epifluorescence microscope (AxioObserver D1; Zeiss, Thornwood, NY) outfitted with an Alpha Plan-Apo 100×/1.46NA objective, temperature- and CO₂₋ controlled environmental chamber, and an LED illuminator (Lumencor Light Engine DAPI/GFP/543/623/690), the motion of fluorescent nanoparticles was captured. 20 s videos (512 × 512, 16-bit image depth) were recorded at a temporal resolution of 66.7 ms using MetaMorph Microscopy Automation and Imaging Software (Molecular Devices, Sunnyvale, CA). The 10 nm spatial resolution (nominal pixel resolution 0.156 µm/pixel) was established previously [29]. Particles were tracked using MATLAB software as described previously [30]. Sub-pixel tracking resolution was realized with light-intensity-weighted averaging of nearby pixels to ascertain the particle center. A mean of $n \ge 40$ -particles/frame (with $n \ge 100$ total traces) were traced for each experiment with 3-4 independent experiments/condition. Time-averaged mean squared displacements (MSD), calculated as $\langle \Delta r^2(\tau) \rangle = [x(t+\tau)$ x(t)]² + [$y(t + \tau) - y(t)$]² (where τ = time scale or time lag) was calculated from the coordinates of particle centers. From this, distributions of MSDs and effective diffusivities (Deff) were computed as previously shown [27]. MSD is also expressed as MSD = $4D_0\tau^{\alpha}$, where α , the slope of the line on a log-log plot, represents the extent of hindrance to particle diffusion ($\alpha = 1$ for pure Brownian diffusion; α < 1 for sub-diffusive motion). Mobile particles were defined as those with $D_{eff} \geq 10^{-1} \; \mu m^2/s$ at τ = 0.2667 s (this τ corresponds to a trajectory length of >5 frames), based on datasets of mobile and immobile nanoparticles (e.g., PS-PEG and PS-COOH nanoparticles) in MG or LAM [14,27]. Theoretical diffusivity in

water was calculated from the Stokes-Einstein equation, as described previously [4,31].

2.5. Dot blotting

To determine antibody affinity to MG, 1 μ L of MG (diluted 1:10 in water), rat anti-mouse laminin-1 IgG $_1$ (AL2, Millipore), or antibiotin antibody was slowly spotted on a nitrocellulose membrane. After the membrane dried, it was blocked in 2% BSA in PBS for 30 min. Membrane with MG dots was incubated for 1 h with either anti-laminin or anti-biotin at 1 μ g/ml in 0.5% BSA, then washed 3 times for 5 min each with 0.05% PBS-Tween 20. All membranes were incubated with goat anti-mouse IgG (HRP-conjugated, 626520, Life Technologies), at a 1:5000 dilution for 1 h in 0.5% BSA, then washed 3 times for 5 min each with 0.05% PBS-Tween 20 and developed with Clarity Western ECL Substrate.

2.6. Salmonella invasion assay

To assay <code>Salmonella</code> invasion, MG (final concentration 2.2 mg/mL) or LAM (final concentration 1.5 mg/mL) with Luria Broth (LB, BD Falcon), BSA, and varying concentrations of anti-<code>Salmonella</code> <code>typhimurium</code> IgG1 (6331; ViroStat) were mixed and incubated for 2 h at 37 °C in the upper chamber of a HTS FluoroBlok MultiWell System with 3.0 µm pores (BD Falcon) in a custom hydration chamber. After confirming mobility in the above-mentioned epifluorescence microscope, GFP-labeled <code>S. typhimurium</code> in 10 µL LB was then added to the top of each well, and 200 µL LB to each well in the bottom chamber. After 2 h of incubation at 37 °C, the top chamber was removed and OD600 in the lower chamber was measured with a SpectraMax M2 (Molecular Devices). Variations included Luria Broth with or without antibody instead of Matrigel® or LAM in the upper chamber. Experiment was performed in triplicate, n = 3.

2.7. Statistics

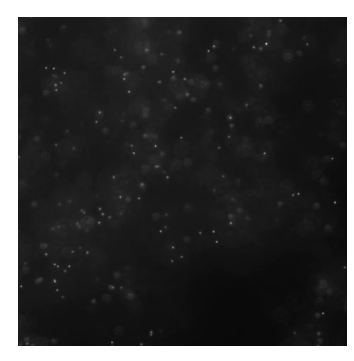
All statistical analysis was performed in GraphPad and was two-sided. MSD data were log-log-transformed and compared within groups using a repeated-measures two-way ANOVA and post hoc Sidák test. Average $D_{\rm eff}$ and % mobile were compared with ANOVA and subsequent Sidák tests. Salmonella invasion data was normalized within each replicate by controlling for background (defined as OD600 of LB only) and maximal invasion of Salmonella in a given matrix. Data were compared within groups using a one-way ANOVA and subsequent Sidák test. In all analyses, global $\alpha = 0.05$. Error bars and \pm represent SEM.

3. Results

Viruses undergo Brownian motion in biogels while evading adhesion [2,10,32]. We prepared densely PEGylated, virus-sized polymeric nanoparticles (PS-PEG) that evade adhesion to biogel constituents to serve as a synthetic mimic of viruses. Using high resolution multiple particle tracking to quantify the diffusion of hundreds of individual nanoparticles in each specimen, we confirmed that nearly all PS-PEG exhibited diffusive Brownian motion in Matrigel[®], slowed only \sim 1.6-fold compared to their theoretical diffusivity in water (Movie S1: Fig. S1). In contrast, similarly sized carboxyl-modified polystyrene nanoparticles (PS-COOH) were extensively immobilized in the same specimen, with geometrically averaged ensemble effective diffusivities (<D $_{eff}$ >) that are $\sim 4000\text{-}$ fold reduced on average compared to PS-PEG (Movie S2; Fig. S1; p < 0.0018). Only 0.2% \pm 0.09% of PS-COOH beads were classified as mobile (possessing $< D_{eff} > in excess of 10^{-1} \mu m^2/s$) vs. 97% ± 1.6% for PS-PEG beads. The effective immobilization of PS-COOH but not PS-PEG nanoparticles confirms Matrigel® affords a sufficiently rigid matrix that can immobilize virus-sized nanoparticles by adhesive interactions, and that PS-PEG nanoparticles can effectively evade adhesive interactions with the biogel constituents.

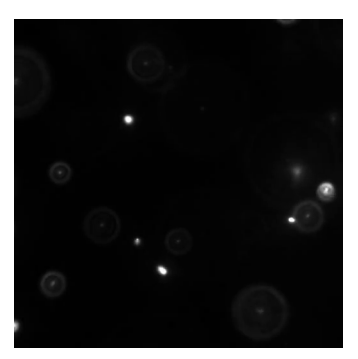


Video S1.



Video S2.

We next assessed whether we can selectively tune the barrier properties of Matrigel® simply by introducing antigen-specific antibodies, using IgG that specifically bind PEG as model antibody. In contrast to the typical high affinity of antibody-antigen bonds (e.g. anti-laminin and laminin), the affinity between typical antibodies with Matrigel® appears very low, virtually undetectable in dot blot assays (Fig. S2). Despite this seemingly negligible affinity, in Matrigel® that contains a final concentration of 10 μg/mL anti-PEG IgG, the <D $_{eff}$ > for PS-PEG (Movie S3) was reduced \sim 167-fold compared to control anti-biotin IgG (Movie S4; Fig. 1d), and the mobile nanoparticle fraction was reduced from 96 ± 0.7% in control IgG to 13 ± 4.2% (p = 0.018; Fig. 1e). Anti-PEG IgG enabled substantial trapping of PS-PEG at 5 μg/mL (Fig. 1), but not at 1 μg/mL (data not shown). The appearance of the PS-PEG nanoparticles, as seen in microscopy videos, remained identical between control IgG and anti-PEG IgG conditions, indicating that the impeded motion of the nanoparticles was not attributed to anti-PEG IgG crosslinking multiple nanoparticles together.



Video S3.

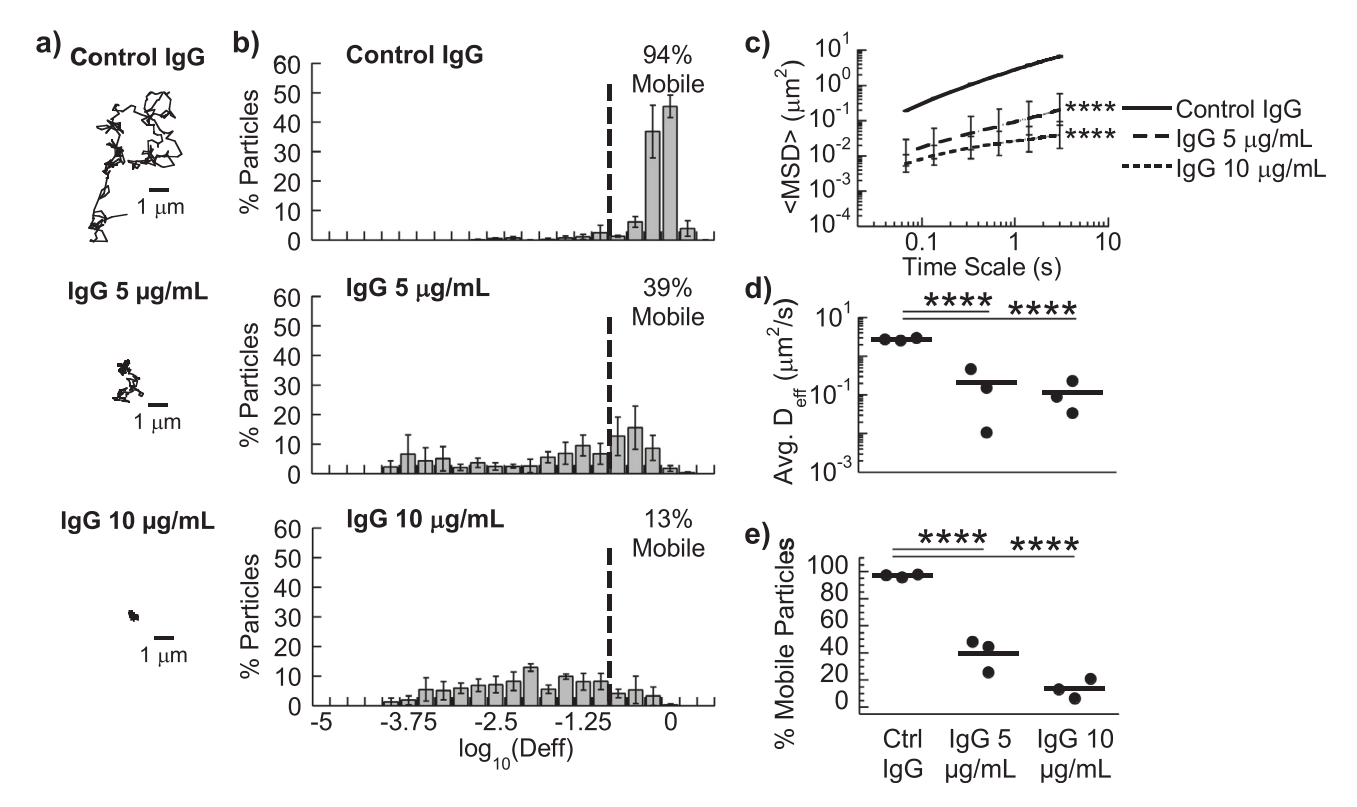
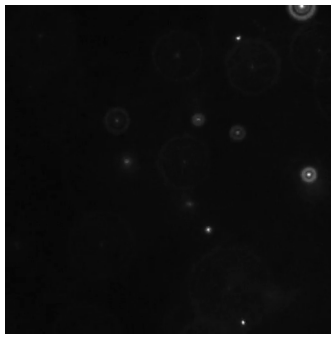


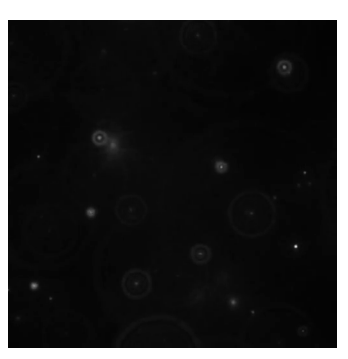
Fig. 1. Anti-PEG IgG antibodies trap 200 nm PEG-coated nanoparticles in MG. (A) Representative traces in MG with 10 μg/mL control IgG or anti-PEG IgG (5 or 10 μg/mL). (B) Distribution of effective diffusivities of nanoparticles under different conditions. (C) Ensemble averaged mean squared displacements (<MSD >) over time. ***** p < 0.0001 compared to Control IgG by two-way RM ANOVA with post hoc Šidák test. (D) Average ensemble effective diffusivities ($<D_{eff} >$) at a time scale of 1 s. (E) Fraction of mobile nanoparticles. For (D) & (E) ***** p < 0.0001 compared to Control IgG by one-way ANOVA with post hoc Šidák test. Error bars represent SEM.



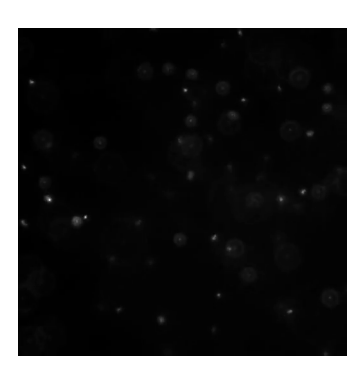
Video S4.

To further confirm the antigen specificity and ability to reinforce barrier properties against different antigens, we mixed in nanoparticles conjugated with biotin-PEG, and found they were effectively immobilized in Matrigel® treated with anti-biotin IgG (Fig. S3). To demonstrate the ability of antigen-specific IgG to mediate trapping even in the presence of large quantities of other IgG crosslinkers, we further evaluated the mobility of PS-PEG in Matrigel® simultaneously treated with both 10 µg/mL anti-PEG IgG and 100-fold excess anti-biotin IgG (i.e. 1 mg/mL) that trapped biotin-PEG beads. We found no appreciable reduction in the trapping potency of anti-PEG IgG despite the excess levels of other antigen-specific IgG (Fig. S4). These results underscore that antigen-specific IgG can robustly immobilize virus-sized nanoparticles in Matrigel® and that this strategy can likely accommodate trapping of a large number of diverse nanoparticle species without compromising the ability to trap any individual foreign species.

We hypothesized that crosslinkers with slightly greater antigen avidity as well as slightly greater affinity to the matrix constituents should facilitate more potent immobilization. IgM, due to its pentameric structure, possesses markedly greater overall binding avidity than IgG [33]. IgM was previously shown to possess slightly greater affinity to mucins than IgG [10]. In good agreement with our expectation, anti-PEG IgM exhibited greater trapping potency, immobilizing a similar fraction of PS-PEG as anti-PEG IgG but at substantially lower concentrations (Fig. 2a and b; Movie S5). The $\langle D_{eff} \rangle$ of PS-PEG was reduced by \sim 90-fold and 137-fold at 5 µg/mL and 3 µg/mL anti-PEG IgM, respectively, compared to control (Fig. 2c; Movie S6). Surprisingly, despite the common assumption that IgM can mediate efficient agglutination, we did not observe appreciable nanoparticle agglutination in Matrigel with anti-PEG IgM (Movie S5).

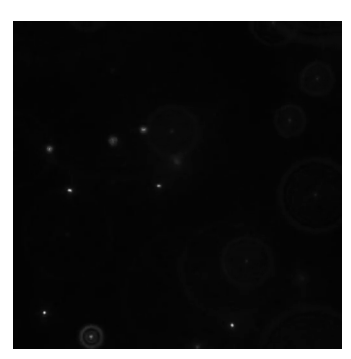


Video S5.



Video S6.

Since many antibody-effector functions are influenced by N-glycans on IgG-Fc [33,34], we speculate that N-glycans on Fc may be responsible for IgG's affinity with Matrigel® constituents. We deglycosylated anti-PEG IgG and IgM with PNGase F and found that the removal of N-glycans substantially reduced the trapping potency of IgG (Movie S7) and IgM (Movie S8). The fraction of mobile nanoparticles increased from $13 \pm 4.2\%$ to $57 \pm 5.3\%$ for IgG (p = 0.0006) and from $13 \pm 6.7\%$ to $67 \pm 9.4\%$ for IgM (0 < 0.0001; Fig. S5).



Video S7.



Video S8.

We next sought to evaluate the extent to which specific components of Matrigel[®] participate in antibody-mediated trapping. By mass, Matrigel[®] is composed 60% of laminin, 30% of collagen IV, and 8% of entactin (or nidogen). Laminin is a high molecular weight glycoprotein that is crosslinked primarily by entactin (or nidogen) in a 1:1 M ratio [7]. In biogels composed of laminin/entactin (LAM),

we observe comparable trapping of nanoparticles by anti-PEG IgG (Movies S9 and S10) and IgM antibodies (Movies S11 and S12): the <D_{eff}> of PS-PEG was reduced \sim 20-fold and \sim 40-fold in anti-PEG IgG- and IgM- treated LAM compared to corresponding controls, respectively (Fig. 3). The collagen IV (COL) found in Matrigel® is a triple helix composed of α_1 and α_2 chains, components of the undifferentiated basement membrane found from early in development [35], and does not contain the more highly cross-linked $\alpha_3\alpha_4\alpha_5$ heterotrimer of the glomerular basement membrane, leading to reduced rigidity and larger pore sizes [36]. In COL biogels, anti-PEG IgG failed to trap nanoparticles (Supplemental Fig. S5): there was no appreciable difference in <D_{eff}> in Collagen IV with and without antibody, suggesting Collagen IV does not directly participate in IgG-matrix interactions.



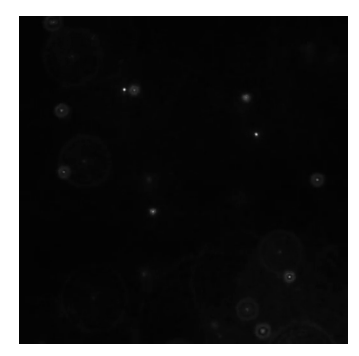
Video S9.



Video S10.



Video S11.



Video S12.

Finally, we evaluated whether specific IgG can reinforce the barrier properties of Matrigel® against even highly motile Salmonella typhimurium. We first added Matrigel® or LAM along with different IgG to the upper chamber of a transwell system and allowed the gel to form, followed by the addition of motile fluorescent Salmonella, and monitored the amount of bacteria that entered the bottom chamber. Anti-LPS IgG markedly reduced the invasion of Salmonella through MG in a dose-dependent manner, with >70% reduction in the fraction of Salmonella that entered the bottom

compartment at an IgG doses of 10 μ g/mL and >93% reduction at an IgG dose of 25 μ g/mL (Fig. 4). We observed a similar extent of reduction of bacterial invasion by *Salmonella*-binding IgG in LAM gels.

4. Discussion

By using third-party crosslinkers that can be adapted to specific antigens of interest, we demonstrate for the first time that the barrier properties of extracellular matrices can be tuned without perturbing the underlying matrix itself. When coupled to our earlier elucidation of IgG interactions with mucin [32,37], our findings suggest antibodies may broadly interact with the matrices of various biogels to create a universal mechanism enabling an effective and highly tunable diffusional barrier against a diverse array of pathogens and foreign particulates. Indeed, this study marks the first example of characterizing IgG and IgM-mediated trapping in native, unmodified extracellular matrix. Previously, we used biotinylated Matrigel to demonstrate that high affinity bonds between antibodies and matrix surprisingly reduce overall trapping potency [26]. The current work is markedly distinct on several fronts, including: 1) work with native, non-mucosal extracellular matrices; 2) comparison of trapping potency of IgM vs. IgG; 3) discovery that laminin, not collagen, is the predominant matrix ele-

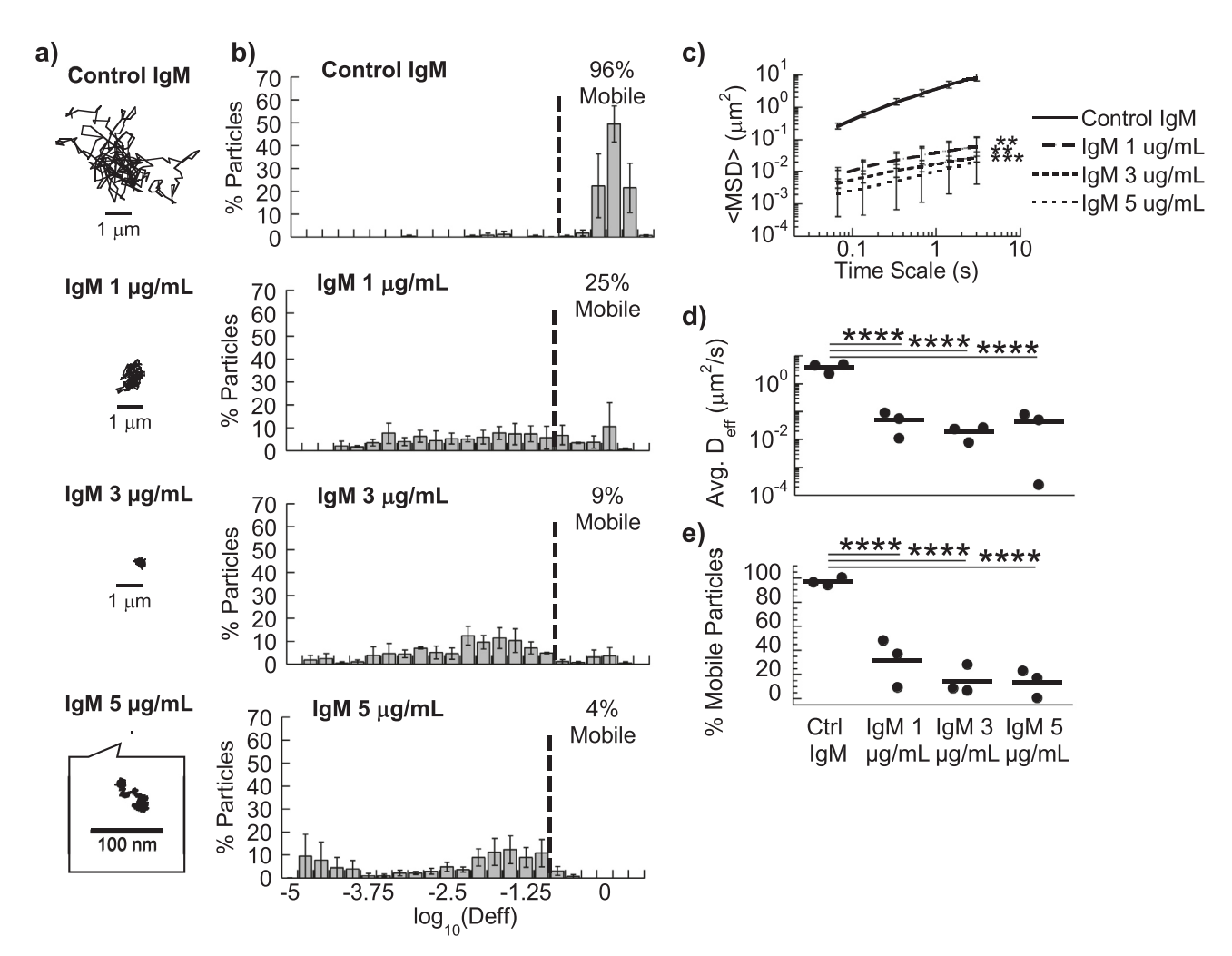


Fig. 2. Anti-PEG IgM antibodies trap 200 nm PEG-coated nanoparticles in MG. (A) Representative traces in MG with $5 \mu g/mL$ control IgM or anti-PEG IgM (1, 3 or $5 \mu g/mL$). (B) Distribution of effective diffusivities of nanoparticles under different conditions. (C) Ensemble averaged mean squared displacements (<MSD >) over time. *** p < 0.01; ****p < 0.001 compared to Control IgM by two-way RM ANOVA with post hoc Šidák test. (D) Average ensemble effective diffusivities (<Deff >) at a time scale of 1 s. (E) Fraction of mobile nanoparticles. For (D) & (E), **** p < 0.0001 compared to Control IgM by one-way ANOVA with post hoc Šidák test. Error bars represent SEM.

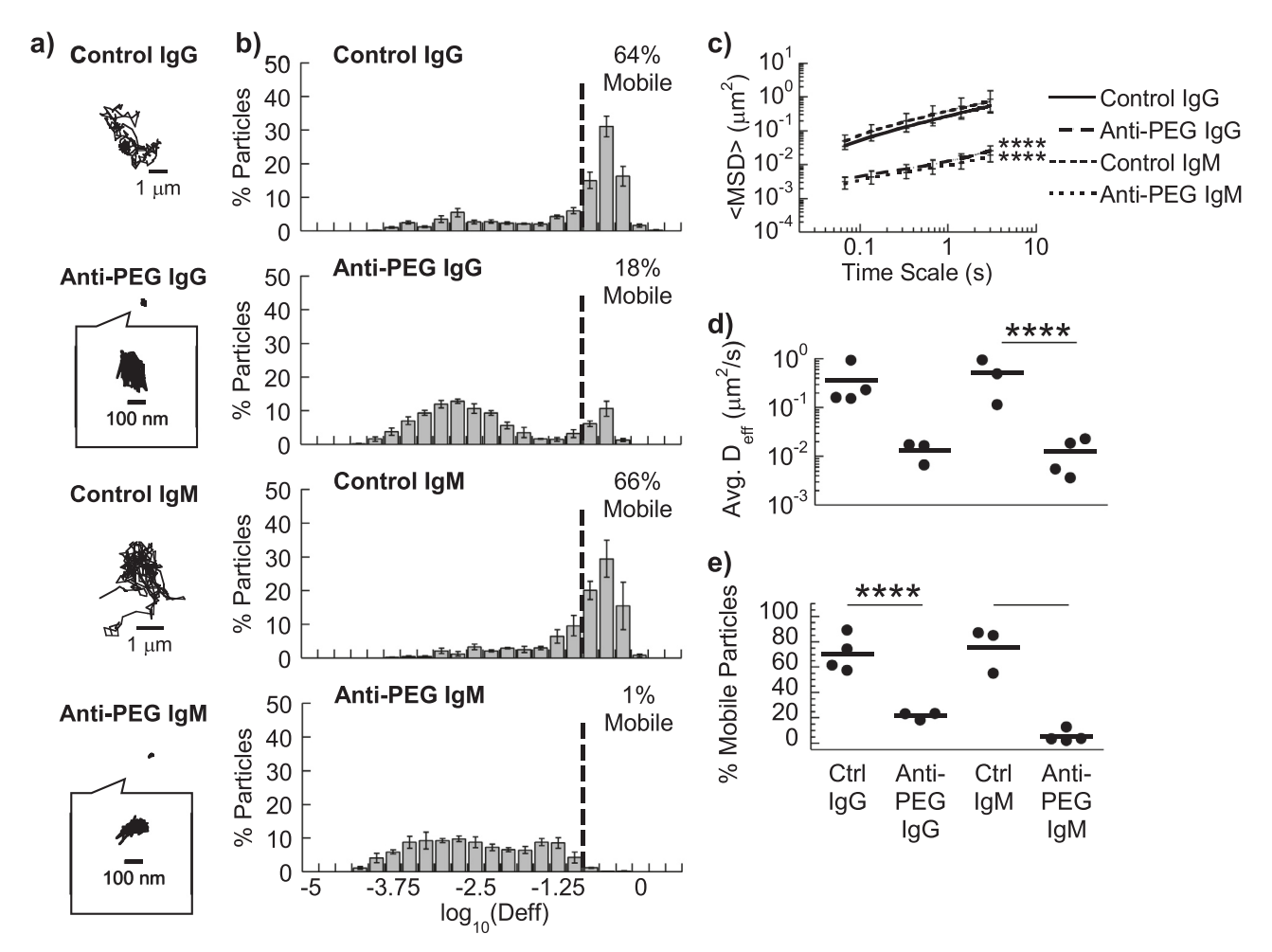


Fig. 3. Anti-PEG IgG and IgM antibodies trap 200 nm PEG-coated nanoparticles in LAM. (A) Representative traces in LAM with control IgG/IgM or anti-PEG IgG/IgM. (B) Distribution of effective diffusivities of nanoparticles under different conditions. (C) Ensemble averaged mean squared displacements (<MSD >) over time. ***** p < 0.0001 compared to corresponding control by two-way RM ANOVA with post hoc Šidák test at every time point. (D) Average ensemble effective diffusivities (<Deff >) at a time scale of 1 s. (E) Fraction of mobile nanoparticles. For (D) & (E), ****p < 0.001; ******p < 0.0001 compared to corresponding control by one-way ANOVA with post hoc Šidák test. Error bars represent SFM.

ment facilitating Ab-mediated trapping in Matrigel; and 4) the finding that this trapping mechanism is potent against even highly motile bacteria. The modular nature of antibody-matrix interactions allows the barrier properties of hydrogels to be dynamically tuned with molecular specificity despite the relatively static biochemistries of most biogels, simply through tailoring specific Ab crosslinkers. The principles laid down here substantially expand our ability to alter the barrier properties of hydrogels.

The observed trapping by IgG and IgM is not caused by nonspecific accumulation of antibodies on nanoparticles or nonspecific alterations of the biogel microstructure, since control IgG and IgM did not slow the mobility of nanoparticles. While antibodies accumulated on the surface of nanoparticles will invariably increase the hydrodynamic diameter of the antibody-nanoparticle complex, the small increase cannot account for the 10-100 + -fold reduction in nanoparticle mobility. Indeed, smaller antibody-nanoparticle complexes were slowed to a much greater extent than larger nanoparticles in biogel, as shown by the potent trapping of ~100 nm PS-PEG by anti-PEG IgG (Fig. 1) compared to the relatively unimpeded motion of ~200 nm PS-PEG in Matrigel® treated with control IgG (Fig. S4). Antibodies can also agglutinate nanoparticles into aggregates far larger than the mesh spacing of the hydrogel. However, no agglutination was observed. Thus, the observed immobilization of nanoparticles must be attributed to adhesive interactions between the array of nanoparticle-bound antibodies and the biogel matrix. Such interactions also limit the ability for particles to collide, a necessary condition to form aggregates.

The notion that antibodies can be harnessed to selectively tune the barrier properties of biogels was likely overlooked in part because interactions between antibodies and biogel constituents are exceedingly weak and transient. For example, the diffusion of IgG and IgM in mucus is slowed only \sim 10-20 and \sim 30-50% relative to their speeds in water [10,38], respectively, which suggests that the bonds between individual antibodies and mucins are sufficiently weak that they are readily broken by thermal excitation. Such weak bonds imply a single antibody is likely incapable of crosslinking a pathogen or particle to mucus. Nevertheless, this weak affinity allows the antibodies to undergo rapid diffusion in hydrogel [26,39-41], and thus quickly accumulate on the surface of nanoparticles and pathogens. In turn, once a critical threshold of antibodies is reached, the array of bound antibodies ensures there is at least one bond between the biogel matrix and nanoparticle-antibody complex at any moment in time, resulting in nanoparticle trapping with permanent avidity [26]. With such a mechanism of immobilization, high affinity bonds between antibodies and the matrix constituents can actually limit the rate of antibody accumulation on the particle surface, and consequently reduce the overall immobilization potency.

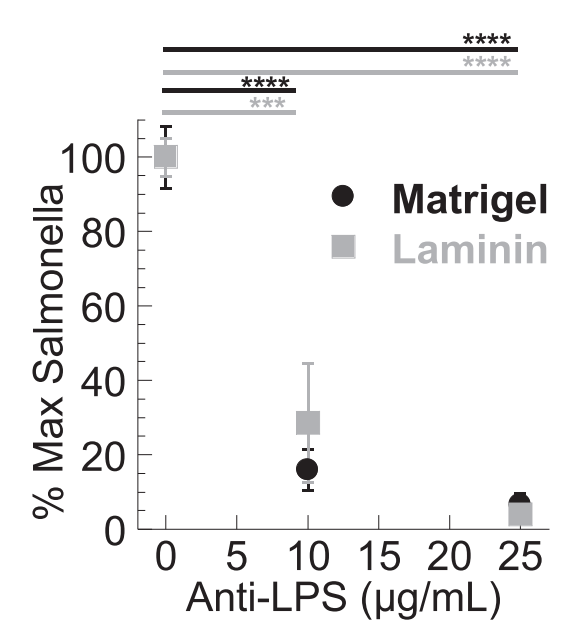


Fig. 4. IgG anti-Salmonella typhimurium in MG and LAM impairs the invasion of Salmonella in a transwell experiment. OD600 of Salmonella in bottom well was normalized to OD600 of media alone and of Salmonella through biogel without antibody. MG: n=4 independent experiments done in triplicate; LAM: n=3 independent experiments done in triplicate. **** p < 0.001; ***** p < 0.001 compared to control by one-way ANOVA with post hoc Šidák test. Error bars represent SEM.

The minimal number of nanoparticle-bound antibodies remains unclear, as does the corresponding nanoparticle size needed to facilitate effective immobilization in different biogels. We recently found that HIV virus-like particles, which have few surface Env glycoproteins [42], could be effectively immobilized by monoclonal anti-gp120 IgG antibodies (unpublished observations), suggesting that as few as one- to two- dozen bound antibodies may be sufficient for immobilization. It is possible that even smaller nanoparticles (diameter < ~100 nm) can be effectively immobilized as long as there is sufficient number of bound antibodies. We hypothesize that optimization of crosslinkers used to mediate trapping, a concept we have discussed in more detail elsewhere [26,42], could reduce the minimum threshold for bound antibodies. Finally, we are actively investigating the specific chemical moieties on the biogel matrix that participate in antibody-mediated trapping to further motivate and support the use of third-party antibody-based crosslinkers for tuning the barrier properties of hydrogels with molecular precision.

5. Data availability

The datasets generated during and/or analyzed during the current study are available from the corresponding author on reasonable request.

6. Code availability

Particle trajectories were analyzed using a MATLAB version of open source particle tracking code, originally developed in IDL by Crocker and Hoffman³⁰. We have adapted this code to analyze particle trajectories on a 'frame-by-frame' basis, as described previously³¹.

Author contributions

J.L.S. and S.K.L. conceptualized the study, designed the experiments, analyzed the data, and wrote the paper; J.L.S. and A.M. per-

formed the experiments. J.M. prepared PEG-conjugated nanoparticles.

Acknowledgements

This work was supported by Eshelman Institute for Innovation, National Institutes of Health (http://www.nih.gov/; Grants R21EB017938 (S.K.L.); the National Science Foundation CAREER Award DMR-1810168 (S.K.L.); the David and Lucile Packard Foundation (http://www.packard.org/; Grant 2013-39274; S.K.L.); and PhRMA Foundation Predoctoral Fellowship (J.L.S.). The funders had no role in study design, data collection and analysis, decision to publish, or preparation of the manuscript.

Disclosures

Mucommune LLC seeks to harness antibody-mucin interactions to improve protection against or treatment of infections at mucosal surfaces, and has licensed intellectual property from the University of North Carolina - Chapel Hill (UNC-CH). SKL is a founder of Mucommune and owns company stock. SKL's relationship with Mucommune is subject to certain restrictions under University policy. The terms of this arrangement are being managed by UNC-CH in accordance with its conflict of interest policies.

Appendix A. Supplementary data

Supplementary data to this article can be found online at https://doi.org/10.1016/j.actbio.2019.03.023.

References

- [1] S.K. Lai, Y.-Y. Wang, D. Wirtz, J. Hanes, Micro- and macrorheology of mucus, Adv. Drug Del. Rev. 61 (2) (2009) 86–100.
- [2] O. Lieleg, K. Ribbeck, Biological hydrogels as selective diffusion barriers, Trends Cell Biol. 21 (9) (2011) 543–551.
- [3] R. Bansil, B.S. Turner, The biology of mucus: Composition, synthesis and organization, Adv. Drug Del. Rev. 124 (2018) 3–15.
- [4] Y. Cu, W.M. Saltzman, Mathematical modeling of molecular diffusion through mucus, Adv. Drug Del. Rev. 61 (2) (2009) 101–114.
- [5] J. Hansing, C. Ciemer, W.K. Kim, X. Zhang, J.E. DeRouchey, R.R. Netz, Nanoparticle filtering in charged hydrogels: Effects of particle size, charge asymmetry and salt concentration, Eur. Phys. J. E Soft Matter 39 (5) (2016) 53.
- [6] T. Stylianopoulos, M.-Z. Poh, N. Insin, M.G. Bawendi, D. Fukumura, L.L. Munn, R. K. Jain, Diffusion of particles in the extracellular matrix: The effect of repulsive electrostatic interactions, Biophys. J. 99 (5) (2010) 1342–1349.
- [7] H.K. Kleinman, G.R. Martin, Matrigel: basement membrane matrix with biological activity, Semin. Cancer Biol. 15 (5) (2005) 378–386.
- [8] H.K. Kleinman, M.L. McGarvey, J.R. Hassell, V.L. Star, F.B. Cannon, G.W. Laurie, G.R. Martin, Basement membrane complexes with biological activity, Biochemistry 25 (2) (1986) 312–318.
- [9] Corning® Matrigel® Matrix: Frequently Asked Questions. https://www.corning.com/media/worldwide/cls/documents/CLS-DL-CC-026 DL.pdf>, (accessed November 8, 2018.).
- [10] S.S. Olmsted, J.L. Padgett, A.I. Yudin, K.J. Whaley, T.R. Moench, R.A. Cone, Diffusion of macromolecules and virus-like particles in human cervical mucus, Biophys. J. 81 (2001) 1930–1937.
- [11] S.K. Lai, K. Hida, S. Shukair, Y.-Y. Wang, A. Figueiredo, R. Cone, T.J. Hope, J. Hanes, Human immunodeficiency virus type 1 is trapped by acidic but not by neutralized human cervicovaginal mucus, J. Virol. 83 (21) (2009) 11196–11200
- [12] L. Tomasetti, M. Breunig, Preventing obstructions of nanosized drug delivery systems by the extracellular matrix, Adv. Healthcare Mater. 7 (3) (2018) 1700739
- [13] J.G. Dancy, A.S. Wadajkar, C.S. Schneider, J.R.H. Mauban, G.F. Woodworth, J.A. Winkles, A.J. Kim, Non-specific binding and steric hindrance thresholds for penetration of particulate drug carriers within tumor tissue, J. Control. Release 238 (2016) 139–148.
- [14] S.K. Lai, Y.-Y. Wang, K. Hida, R. Cone, J. Hanes, Nanoparticles reveal that human cervicovaginal mucus is riddled with pores larger than viruses, Proc. Natl. Acad. Sci. U. S. A. 107 (2) (2010) 598–603.
- [15] O. Chaudhuri, S.T. Koshy, C. Branco da Cunha, J.-W. Shin, C.S. Verbeke, K.H. Allison, D.J. Mooney, Extracellular matrix stiffness and composition jointly regulate the induction of malignant phenotypes in mammary epithelium, Nat. Mater. 13 (10) (2014) 970–978.

- [16] N. Bodenberger, D. Kubiczek, L. Trösch, A. Gawanbacht, S. Wilhelm, D. Tielker, F. Rosenau, Lectin-mediated reversible immobilization of human cells into a glycosylated macroporous protein hydrogel as a cell culture matrix, Sci. Rep. 7 (1) (2017) 6151.
- [17] T.V. Updyke, G.L. Nicolson, Immunoaffinity isolation of membrane antigens with biotinylated monoclonal antibodies and immobilized streptavidin matrices, J. Immunol. Methods 73 (1984) 83–95.
- [18] T. Miyata, N. Asami, T. Uragami, A reversibly antigen-responsive hydrogel, Nature 399 (1999) 766–769.
- [19] C.M. Soto, C.H. Patterson, P.T. Charles, B.D. Martin, M.S. Spector, Immobilization and hybridization of DNA in a sugar polyacrylate hydrogel, Biotechnol. Bioeng. 92 (7) (2005) 934–942.
- [20] H.-J. Kim, K. Zhang, L. Moore, D. Ho, Diamond nanogel-embedded contact lenses mediate lysozyme-dependent therapeutic release, ACS Nano 8 (3) (2014) 2998–3305.
- [21] J.P. Best, J. Cui, M. Müllner, F. Caruso, Tuning the mechanical properties of nanoporous hydrogel particles via polymer cross-linking, Langmuir 29 (31) (2013) 9824–9831.
- [22] Y. Kim, A.Y. Abuelfilat, S.P. Hoo, A. Al-Abboodi, B. Liu, T. Ng, P. Chan, J. Fu, Tuning the surface properties of hydrogel at the nanoscale with focused ion irradiation, Soft Matter 10 (42) (2014) 8448–8456.
- [23] S. Santhanam, J. Liang, J. Struckhoff, P.D. Hamilton, N. Ravi, Biomimetic hydrogel with tunable mechanical properties for vitreous substitutes, Acta Biomater. 43 (2016) 327–337.
- [24] W.S. Toh, T.C. Lim, M. Kurisawa, M. Spector, Modulation of mesenchymal stem cell chondrogenesis in a tunable hyaluronic acid hydrogel microenvironment, Biomaterials 33 (15) (2012) 3835–3845.
- [25] K.M. Mabry, M.E. Schroeder, S.Z. Payne, K.S. Anseth, Three-dimensional high-throughput cell encapsulation platform to study changes in cell-matrix interactions, ACS Appl. Mater. Interfaces 8 (34) (2016) 21914–21922.
- [26] J. Newby, J.L. Schiller, T. Wessler, J. Edelstein, M.G. Forest, S.K. Lai, A blueprint for robust crosslinking of mobile species in biogels with weakly adhesive molecular anchors, Nat. Commun. 8 (1) (2017) 833.
- [27] S.K. Lai, D.E. O'Hanlon, S. Harrold, S.T. Man, Y.-Y. Wang, R. Cone, J. Hanes, Rapid transport of large polymeric nanoparticles in fresh undiluted human mucus, Proc. Natl. Acad. Sci. U. S. A. 104 (5) (2007) 1482–1487.
- [28] Q. Yang, S.W. Jones, C.L. Parker, W.C. Zamboni, J.E. Bear, S.K. Lai, Evading immune cell uptake and clearance requires PEG grafting at densities substantially exceeding the minimum for brush conformation, Mol. Pharm. 11 (4) (2014) 1250–1258.
- [29] J. Apgar, Y. Tseng, E. Federov, M.B. Herwig, S.C. Almo, D. Wirtz, Multiple-particle tracking measurements of heterogeneities in solutions of actin filaments and actin bundles, Biophys. J. 79 (2) (2000) 1095–1106.

- [30] Y.-Y. Wang, K.L. Nunn, D. Harit, S.A. McKinley, S.K. Lai, Minimizing biases associated with tracking analysis of submicron particles in heterogeneous biological fluids, J. Control. Release 220 (Pt A) (2015) 37–43.
- [31] M. Dawson, D. Wirtz, J. Hanes, Enhanced viscoelasticity of human cystic fibrotic sputum correlates with increasing microheterogeneity in particle transport, J. Biol. Chem. 278 (50) (2003) 50393–50401.
- [32] Y.-Y. Wang, A. Kannan, K.L. Nunn, M.A. Murphy, D.B. Subramani, T.R. Moench, R.A. Cone, S.K. Lai, IgG in cervicovaginal mucus traps HSV and prevents vaginal herpes infections, Mucosal Immunol. 7 (5) (2014) 1036–1044.
- [33] L.L. Lu, T.J. Suscovich, S.M. Fortune, G. Alter, Beyond binding: antibody effector functions in infectious diseases, Nat. Rev. Immunol. 18 (1) (2018) 46–61.
- [34] A. Russell, E. Adua, I. Ugrina, S. Laws, W. Wang, Unravelling immunoglobulin G Fc N-glycosylation: a dynamic marker potentiating predictive, preventive and personalised medicine, Int. J. Mol. Sci. 19 (390) (2018).
- [35] P.G. Robey, G.R. Martin, Type IV collagen contains two distinct chains in separate molecules, Coll. Relat. Res. 1 (1) (1980) 27–38.
- [36] K.L. Brown, C.F. Cummings, R.M. Vanacore, B.G. Hudson, Building collagen IV smart scaffolds on the outside of cells, Protein Sci. 26 (11) (2017) 2151– 2161.
- [37] C.E. Henry, Y.-Y. Wang, Q. Yang, T. Hoang, S. Chattopadhyay, T. Hoen, L.M. Ensign, K.L. Nunn, H. Schroeder, J. McCallen, T. Moench, R. Cone, S.R. Roffler, S. K. Lai, Anti-PEG antibodies alter the mobility and biodistribution of densely PEGylated nanoparticles in mucus, Acta Biomater. 43 (2016) 61–70.
- [38] W.M. Saltzman, M.L. Radomsky, K.J. Whaley, R.A. Cone, Antibody diffusion in human cervical mucus, Biophys. J. 66 (1994) 506–515.
- [39] A. Chen, S.A. McKinley, S. Wang, F. Shi, P.J. Mucha, M.G. Forest, S.K. Lai, Transient antibody-mucin interactions produce a dynamic molecular shield against viral invasion, Biophys. J. 106 (9) (2014) 2028–2036.
- [40] S.A. McKinley, A. Chen, F. Shi, S. Wang, P.J. Mucha, M.G. Forest, S.K. Lai, Modeling neutralization kinetics of HIV by broadly neutralizing monoclonal antibodies in genital secretions coating the cervicovaginal mucosa, PLoS ONE 9 (6) (2014) e100598.
- [41] H.A. Schroeder, K.L. Nunn, A. Schaefer, C.E. Henry, F. Lam, M.H. Pauly, K.J. Whaley, L. Zeitlin, M.S. Humphrys, J. Ravel, S.K. Lai, Herpes simplex virus-binding IgG traps HSV in human cervicovaginal mucus across the menstrual cycle and diverse vaginal microbial composition, Mucosal Immunol. (2018).
- [42] T. Wessler, A. Chen, S.A. McKinley, R. Cone, M.G. Forest, S.K. Lai, Using computational modeling to optimize the design of antibodies that trap viruses in mucus, ACS Infect. Dis. 2 (1) (2016) 82–92.